JACS
JOURNAL OF THE AMERICAN CHEMICAL SOCIETY

Communication

pubs.acs.org/JACS

Highly Monodisperse M^{III}-Based soc-MOFs (M = In and Ga) with Cubic and Truncated Cubic Morphologies

Maolin Pang,[†,‡] Amy J. Cairns,[†] Yunling Liu,[†] Youssef Belmabkhout,[†] Hua Chun Zeng,*[,‡] and Mohamed Eddaoudi*[,†]

[†]Advanced Membrane and Porous Materials Center, King Abdullah University of Science and Technology, Thuwal 23955-6900, Kingdom of Saudi Arabia

[‡]Department of Chemical and Biomolecular Engineering and KAUST-NUS GCR Program, Faculty of Engineering, National University of Singapore, 10 Kent Ridge Crescent, Singapore

Supporting Information

ABSTRACT: In this work, we carry out an investigation on shape-controlled growth of In^{III}- and Ga^{III}-based square-octahedral metal−organic frameworks (**soc**-MOFs). In particular, controllable crystal morphological evolution from simple cubes to complex octadecahedra has been achieved, and resultant highly uniform crystal building blocks promise new research opportunities for preparation of self-assembled MOF materials and related applications.

Over the past two decades, metal−organic frameworks (MOFs) have received immense attention owing to their hybrid composition, modularity, ultrahigh surface areas and tunable porosity, and numerous potential applications.[1−8] Compared to considerable work on synthesis, shape-controlled growth (or morphogenesis) of MOFs has been largely overlooked; the situation is quite different from other nanomaterials developments, such as semiconductor quantum dots and nanoparticles of transition metal oxides and noble metals, where particulate monodispersity and shape controllability have been focal points for research. Recently, downsizing of MOF crystals/particles into the nano- or micrometer regime has gradually attracted more attention from the research community.[6−9] The ability to deliberately access monodisperse nano- or microsized MOFs, with controlled crystal size and morphology, offers prospective applications in heterogeneous catalysis, porous membranes, thin-film devices, biomedical imaging and biosensing, and controlled drug release, among others.[6−11] To date, research groups have successfully prepared nano- or microscaled MOFs by employing various methods such as room-temperature precipitation,[12−14] reverse microemulsion,[15,16] solvothermal treatment,[17,18] microwave-assisted process,[19] and coordination modulation.[20,21] However, to the best of our knowledge, shape-controlled growth of highly monodisperse MOF crystals in the sub-micrometer regime has not been realized so far. In addition, detailed studies on the manipulation and formation of MOF materials under complex synthetic conditions are scarce.[9−11] Herein we present the controlled morphogenesis and self-assembly of MOF crystals. We specifically selected M^{III}-based MOFs ($[M_3O(C_{16}N_2O_8H_6)_{1.5}(H_2O)_3](H_2O)_3(NO_3)$, M = In and Ga) with square-octahedral (**soc**) topology as a starting platform, in view of their high chemical stability and potential applications across various fields.[22−24]

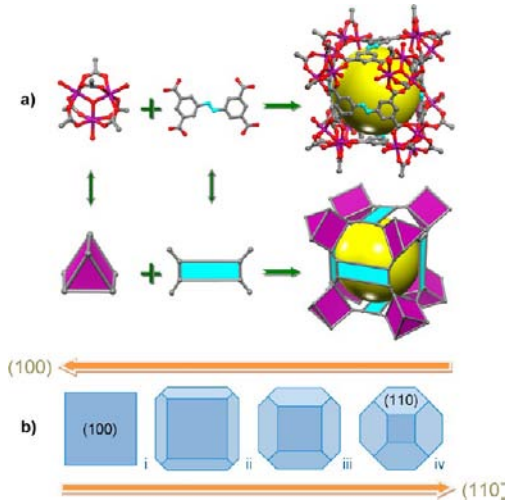

Figure 1. (a) Structure of **soc**-MOF-**1a**: (top) ball-and-stick representation and (bottom) polyhedral representation of the oxygen-centered indium carboxylates trimer molecular building block ($[In_3O(CO_2)_6(H_2O)_3]$, which can be viewed as a 6-connected node having trigonal-prismatic geometry), the organic ligand (ABTC, which is shown as a 4-connected node having rectangular-planar geometry), and the cuboidal cage (In, purple; C, gray; N, light blue; O, red; the cavity space is indicated by the yellow vdW sphere; and hydrogen atoms, water molecules, and NO_3^- ions are omitted for clarity). (b) Morphologies of monodisperse **soc**-MOF-**1a** crystals prepared in this work: (i) normal cube viewed along the [100] axis and (ii−iv) (110)-truncated cubes with increasing surface area of the {110} facets.

The parent In-**soc**-MOF, **soc**-MOF-**1a**, is constructed from oxygen-centered indium carboxylate trimer molecular building blocks linked together through 3,3′,5,5′-azobenzenetetracarboxylic acid (H_4-ABTC) to give a cationic framework (Figure 1a) consisting of two types of interconnected channels (i.e., hydrophobic and hydrophilic), as well as a nanoscale central cage (<1 nm) that encapsulates nitrate anions, balancing the overall framework charge. The unique chemical and structural features of this finely tunable material lead to an exceptional

Received: May 21, 2012
Published: July 19, 2012

   dx.doi.org/10.1021/ja3049282 | J. Am. Chem. Soc. 2012, 134, 13176−13179

hydrogen uptake capacity, which is of potential interest for gas storage and gas separation applications.[22−24] Similarly, it is anticipated that isostructural M^{III}-**soc**-MOF analogues constructed with lighter metal cations (e.g., Al^{3+} and Ga^{3+}) should have an enhanced gravimetric adsorption capacity due to the resultant reduced framework density. Nevertheless, the growth of these isostructural metal−organic hybrids by traditional solvothermal methods has remained unsuccessful. To circumvent this difficulty, we have employed, in this work, a novel solvothermal approach to obtain not only Ga-based **soc**-MOF but also highly monodisperse In- and Ga-based **soc**-MOFs,[17,18] whereby the control of their crystal size and morphology has been virtually (efficiently) achieved (Figure 1b).

In order to obtain highly monodisperse **soc**-MOF-**1a**, a new synthetic protocol was devised in this work where poly(vinylpyrrolidone) (PVP) and tetramethylammonium nitrate (TMAN) or 4,4′-trimethylenedipiperidine (TMDP) were mutually introduced to the reaction medium as surfactant and structure-directing agents (SDAs), respectively (see experimental details in SI). Indeed, the added surfactant and SDAs were able to regulate the growth and thus the morphology of the final products. Figure 2a,b displays representative SEM images of the resulting homogeneous and monodisperse **soc**-MOF-**1a** material with cubic crystal morphology, produced from solvothermal reaction between rectangle-like H_4-ABTC and $In(NO_3)_3{\cdot}xH_2O$ in an acetonitrile (CH_3CN):dimethyl sulfoxide (DMSO):*N*,*N*′-dimethylformamide (DMF) [2:1:1] solution containing TMAN and PVP, whose purity was confirmed by similarities between the experimental and calculated powder X-ray diffraction (PXRD) patterns (SI-3). The resultant **soc**-MOF-**1a** cubes, average diameter estimated at 1.38 ± 0.02 μm, are highly symmetrical (i.e., nearly perfect cubes), terminated with 6 {100} crystal planes (type i, Figure 1b), as opposed to the polyhedral-shaped crystals attained under the original reaction conditions and subsequently used for X-ray single-crystal structure determination.[22]

In order to gain a better understanding of the morphogenesis/reaction conditions relationship in this approach, we investigated the influence of preparative parameters on the size- and shape-controlled crystal growth. Table 1 lists typical quantities of solvent, SDA, and surfactant used in the reaction medium for the construction of monodisperse **soc**-MOF-**1a** crystals. Our initial study was aimed at determining and isolating solvent effects on the crystal morphology, specifically DMSO. In fact, increasing the amount of DMSO from 0.5 to 1.0 mL permitted the formation of highly monodisperse **soc**-MOF-**1a** cubes with relatively reduced size—average edge length around 0.88 ± 0.03 μm (Figure 2c,d). Interestingly, these slightly rounded, sub-micrometer cubes tend to form a close-packed superlattice owing to their high uniformity. To the best of our knowledge, this is a benchmark result and it represents a cutting-edge report pertaining to the assembly and fabrication of two-dimensional superlattice of MOFs without any size-selection process or assistance from patterned templates or lithography methods.

We also examined the role of SDAs in morphological control by increasing the amount of TMAN from 0.01 to 0.10 mL, while keeping all other reaction conditions unaltered. Shown in Figure 2e,f, again, highly uniform **soc**-MOF-**1a** cubes were formed, with an average edge length of 1.5 ± 0.02 μm, which also favor the formation of a superlattice via the "oriented attachment" mechanism.[25−27] It is worth mentioning that the size of the **soc**-MOF-**1a** cubes could be controlled simply by

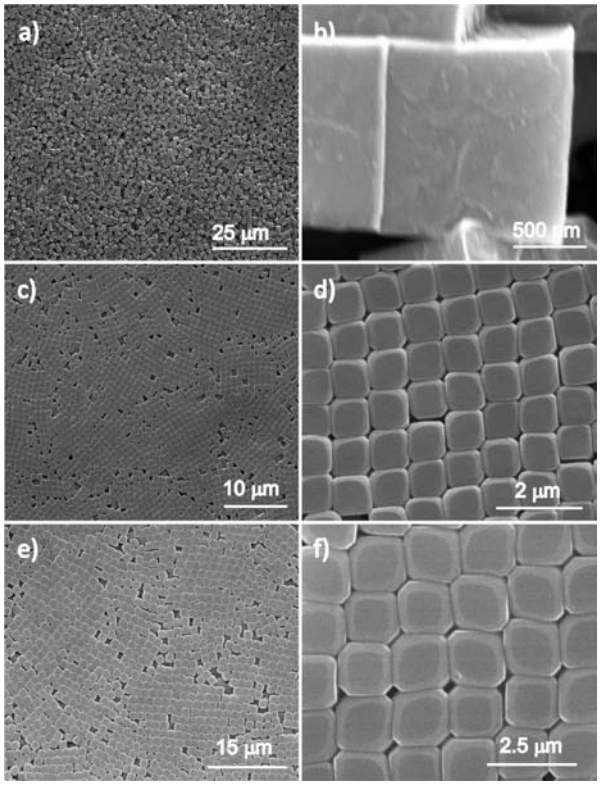

Figure 2. SEM images of **soc**-MOF-**1a** crystals: (a,b) cubes, (c,d) edge- and corner-rounded cubes (TMAN, 0.01 mL), and (e,f) (110)-truncated cubes (TMAN, 0.10 mL) with small {110} facets.

varying the concentration of TMAN in the synthesis; that is, the size of the crystals increased from 0.88 ± 0.03 to 1.50 ± 0.02 μm when the amount of TMAN added was changed from 0.01 to 0.10 mL. Furthermore, the edge- and corner-rounded cubes (shown in Figure 2c,d) at relatively lower concentration could be viewed as a solid intermediate between type i and type ii crystals (Figure 1b; also see SI-3), whereas the {110} facets become more visible in the crystals at higher concentration (Figure 2e,f; i.e., formation of more recognizable octadecahedral crystals, type ii).

Furthermore, we have explored two other synthetic routes in order to assess the synergistic effects of solvents, SDAs, and surfactants in this approach. First, distinct from the preparation of **soc**-MOF-**1a** cubes, DMF was eliminated from the reaction media by dissolving PVP in DMSO instead of DMF, while keeping other experimental conditions constant. The resultant octadecahedra crystals, all comparable in size (about 1.60 ± 0.04 μm), are well-faceted with 6 {100} and 12 {110} crystal planes, as shown in Figure 3a,b (type iii, Figure 1b). Apparently, with this simple solvent adjustment/replacement, the {110} crystal facets can be further stabilized. The slight difference in the solubility profile of PVP in DMSO vs DMF potentially impacts how PVP interacts with the different crystal surfaces. Moreover, the effect is more pronounced with the complete elimination of DMF from the reaction media, indicating synergistic effects among all the reagents involved in the synthesis (SI-3). Additionally, the role of surfactant was explored. In fact, the surfactant is indispensable for size control, as evidenced by the limited regularity of cubes in the absence of PVP.

The second synthetic route investigated herein was the introduction of TMDP as a SDA instead of TMAN, while

dx.doi.org/10.1021/ja3049282 | J. Am. Chem. Soc. 2012, 134, 13176−13179

Table 1. Preparative Parameters of soc-MOF-1a Crystals

sample	DMSO (mL)	CH_3CN (mL)	DMF (mL)	TMAN (mmol)	TMDP (mmol)	PVP (mmol)
Figure 2a,b	0.5	1.0	0.5	7.3×10^{-3}		5×10^{-3}
Figure 2c,d	1.0	1.0	0.5	7.3×10^{-3}		5×10^{-3}
Figure 2e,f	1.0	1.0	0.5	7.3×10^{-2}		5×10^{-3}
Figure 3a,b	1.0	1.0		7.3×10^{-3}		5×10^{-3}
Figure 3c,d	1.0	1.0	0.5		4.8×10^{-3}	5×10^{-3}

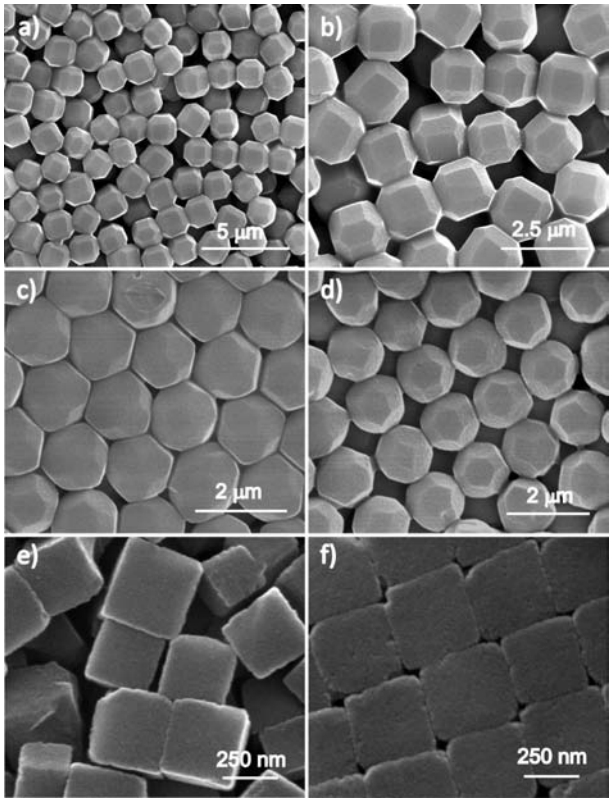

Figure 3. SEM images of (a,b) (110)-truncated cubes of **soc**-MOF-**1a** crystals with large {110} facets, (c,d) (110)-truncated cubes of **soc**-MOF-**1a** crystals with very large {110} facets, (e) irregular cubes of **soc**-MOF-**1b** crystals prepared without surfactant, and (f) uniform cubes of **soc**-MOF-**1b** crystals prepared with assistance of Brij-98. More examples can be found in SI-4.

keeping other process parameters identical. Intriguingly (as shown in Figure 3c,d), the surface area of {110} facets increases significantly in the presence of TMDP (type iv, Figure 1b). It is thus believed that the {110} planes could be stabilized more effectively in the presence of TMDP, though synergistic effects from other organics should not be ignored. The resulting sphere-like single crystals of **soc**-MOF-**1a** are now bounded with 6 small {100} and 12 large {110} planes. Owing to their approximate spherical morphology, the monodisperse **soc**-MOF-**1a** building block crystals can form both hexagonal close-packed and square close-packed assemblies (Figure 3c,d), most of which use their large {110} facets to achieve maximum contacts in the crystal assemblages.

The presented study has permitted us to gain insight into the distinctive and/or cooperative effects of the solvents, SDAs, and surfactants on **soc**-MOF crystal size and shape-controlled growth (morphogenesis): (i) normal **soc**-MOF-**1a** cubes can be prepared by adding small amounts of TMAN (0.1 mL), which can be transformed to edge- and corner-rounded cubes by increasing the amount of DMSO solvent to 1.0 mL; (ii) **soc**-MOF-**1a** with (110)-truncated cubes morphology can be isolated when using DMSO and acetonitrile as cosolvents in the absence of DMF; (iii) introduction of PVP as surfactant in the reaction medium is critical in order to regulate the crystal size of the constructed **soc**-MOF crystals; (iv) the SDAs (TMAN or TMDP), which additionally act as bases and accelerate the reaction via deprotonation of the ligands, are found to impact the resulting **soc**-MOF crystal habits, modulate the crystal growth, and direct the dominant crystal facets.[9,11,22] It should be mentioned that the reaction was largely accelerated by increasing the amount of TMAN from 0.01 to 0.10 mL, and the size for the product was increased from 0.88 ± 0.03 to 1.50 ± 0.02 μm accordingly.

We have extended the above observations and findings to other M^{III}-based **soc**-MOF systems and report, for the first time, the synthesis of the Ga-**soc**-MOF, **soc**-MOF-**1b**. It is of interest to construct Ga-based **soc**-MOF, a relatively lighter framework than the parent In-based **soc**-MOF-**1a**, due to its expected relatively higher specific surface area and potentially enhanced H_2 gravimetric adsorption capacity.

Indeed, **soc**-MOF-**1b** cubes were first prepared in the absence of SDAs or surfactant, and the SEM image of an as-synthesized sample is presented in Figure 3e. The **soc**-MOF-**1b** crystal cubes were predominantly not uniform in the absence of surfactant, with sizes ranging from 200 to 300 nm. So far, attempts to grow relatively large crystals of **soc**-MOF-**1b** suitable for single-crystal X-ray determination were ineffective; therefore, the calculated PXRD pattern from **soc**-MOF-**1a** single-crystal data was used as a reference to confirm the formation and phase purity of the resultant **soc**-MOF-**1b** crystals. As anticipated, the experimental PXRD pattern of **soc**-MOF-**1b** matches the calculated pattern of **soc**-MOF-**1a** (SI-4). This result confirms that Ga-**soc**-MOF, an isostructural analogue of In-**soc**-MOF, has been successfully prepared by this approach.

In order to introduce uniformity in the constructed **soc**-MOF-**1b** cubes, several surfactants were introduced individually into the reaction mixture, such as Brij-98 ($C_{18}H_{35}(OCH_2CH_2)_nOH$, $n \sim 20$), DEG, and PEG 8000. Interestingly, highly monodisperse **soc**-MOF-**1b** cubes, with an average edge length at 360 ± 20 nm, were prepared in the presence of Brij-98, and, as anticipated, a two-dimensional superlattice formed in certain localized areas, as shown in Figure 3f. Similar crystal uniformity was observed in the presence of DEG and PEG-8000, respectively (SI-4).

As our preliminary effort in application of these sub-micrometer MOFs, gas adsorption measurement were conducted on the exchanged and fully evacuated **soc**-MOF-**1a** cubes and **soc**-MOF-**1b** cubes (SI-5). As shown in Figure 4a, the fully reversible type-I argon adsorption isotherms recorded at 87 K confirm permanent microporosity for both activated **soc**-MOF compounds. The apparent Langmuir surface areas and pore volumes for **soc**-MOF-**1b** cubes and **soc**-MOF-**1a** cubes were estimated to be (1510 m^2/g and 0.48 cm^3/g) and

dx.doi.org/10.1021/ja3049282 | J. Am. Chem. Soc. 2012, 134, 13176−13179

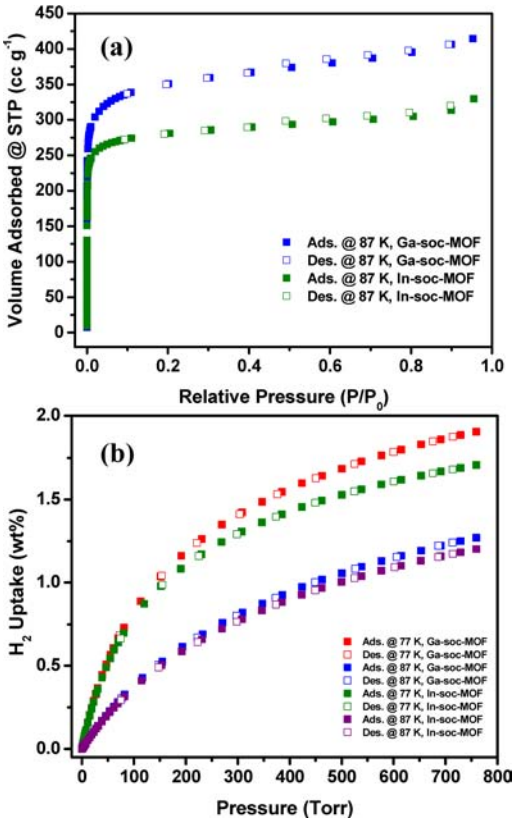

Figure 4. (a) Argon adsorption isotherm at 87 K and (b) hydrogen sorption isotherms at 77 and 87 K for **soc**-MOF-**1a** and **soc**-MOF-**1b** cubes.

(1180 m^2/g and 0.37 cm^3/g), respectively (SI-5). The H_2 uptake capacities for **soc**-MOF-**1b** cubes were evaluated at 87 and 77 K, and found to reach a maximum uptake of 1.27 and 1.91 wt % at one bar, respectively (Figure 4b). As anticipated, owing to the lower framework density for **soc**-MOF-**1b** than that of **soc**-MOF-**1a**, the estimated Langmuir surface area and H_2 uptake capacity of **soc**-MOF-**1b** cubes are indeed higher than those of **soc**-MOF-**1a** cubes. However, the gas uptake values for **soc**-MOF-**1a** cubes were found to be slightly lower than expected, compared to the original **soc**-MOF-**1a** single crystals' sorption data, which can be attributed to residual traces of surfactant. Nevertheless, the isosteric heat of adsorption (Q_{st}; SI-5) for H_2 is in perfect agreement with the **soc**-MOF-**1a** single crystals across the entire studied range. In fact, other researchers have also observed similar phenomena between the nanosized ZIF-8 and its single-crystal form.[13]

In summary, this work is significant for the following aspects. It reports the preparation of highly monodisperse In-**soc**-MOF with tunable crystal morphologies, from simple cubes to complex octadecahedra by a varied solvothermal approach. Large-area superlattices assembled from uniform MOF building units have been achieved. Moreover, the introduced approach has permitted, for the first time, the synthesis of Ga-based **soc**-MOF, in the form of crystal cubes. This work extends the synthetic strategy and methodic versatility for further development of MOFs. The realization of these uniform MOF building block crystals paves the way to new research opportunities for self-assembled MOF materials and their potential applications, including thin films for sensing devices and membranes for gas separations.

■ ASSOCIATED CONTENT

Supporting Information

Experimental details, PXRD spectra, additional SEM images, and gas adsorption data. This material is available free of charge via the Internet at http://pubs.acs.org.

■ AUTHOR INFORMATION

Corresponding Author

chezhc@nus.edu.sg; mohamed.eddaoudi@kaust.edu.sa

Notes

The authors declare no competing financial interest.

■ ACKNOWLEDGMENTS

The authors acknowledge financial support from King Abdullah University of Science and Technology, Saudi Arabia, and National University of Singapore, Singapore.

■ REFERENCES

(1) Ferey, G. *Chem. Soc. Rev.* **2008**, *37*, 191.
(2) Horike, S.; Shimomura, S.; Kitagawa, S. *Nat. Chem.* **2009**, *1*, 695.
(3) Tranchemontagne, D. J.; Mendoza-Cortes, J. L.; O'Keeffe, M.; Yaghi, O. M. *Chem. Soc. Rev.* **2009**, *38*, 1257.
(4) Li, J. R.; Kuppler, R. J.; Zhou, H. C. *Chem. Soc. Rev.* **2009**, *38*, 1477.
(5) Murray, L. J.; Dinca, M.; Long, J. R. *Chem. Soc. Rev.* **2009**, *38*, 1294.
(6) Spokoyny, A. M.; Kim, D.; Sumrein, A.; Mirkin, C. A. *Chem. Soc. Rev.* **2009**, *38*, 1218.
(7) Lin, W. B.; Rieter, W. J.; Taylor, K. M. L. *Angew. Chem., Int. Ed.* **2009**, *48*, 650.
(8) Carne, A.; Carbonell, C.; Imaz, I.; Maspoch, D. *Chem. Soc. Rev.* **2011**, *40*, 291.
(9) Stock, N.; Biswas, S. *Chem. Rev.* **2012**, *112*, 933.
(10) Yanai, N.; Granick, S. *Angew. Chem., Int. Ed.* **2012**, *51*, 5638.
(11) Pan, Y. C.; Heryadi, D.; Zhou, F.; Zhao, L.; Lestari, G.; Su, H. B.; Lai, Z. P. *CrystEngComm* **2011**, *13*, 6937.
(12) Guo, H. L.; Zhu, Y. Z.; Qiu, S. L.; Lercher, J. A.; Zhang, H. J. *Adv. Mater.* **2010**, *22*, 4190.
(13) Cravillon, J.; Munzer, S.; Lohmeier, S. J.; Feldhoff, A.; Huber, K.; Wiebcke, M. *Chem. Mater.* **2009**, *21*, 1410.
(14) Sun, X. P.; Dong, S. J.; Wang, E. K. *J. Am. Chem. Soc.* **2005**, *127*, 13102.
(15) Rieter, W. J.; Taylor, K. M. L.; An, H. Y.; Lin, W. L.; Lin, W. B. *J. Am. Chem. Soc.* **2006**, *128*, 9024.
(16) Rieter, W. J.; Taylor, K. M. L.; Lin, W. B. *J. Am. Chem. Soc.* **2007**, *129*, 9852.
(17) Cho, W.; Lee, H. J.; Oh, M. *J. Am. Chem. Soc.* **2008**, *130*, 16943.
(18) Jung, S.; Oh, M. *Angew. Chem., Int. Ed.* **2008**, *47*, 2049.
(19) Ni, Z.; Masel, R. I. *J. Am. Chem. Soc.* **2006**, *128*, 12394.
(20) Tsuruoka, T.; Furukawa, S.; Takashima, Y.; Yoshida, K.; Isoda, S.; Kitagawa, S. *Angew. Chem., Int. Ed.* **2009**, *48*, 4739.
(21) Umemura, A.; Diring, S.; Furukawa, S.; Uehara, H.; Tsuruoka, T.; Kitagawa, S. *J. Am. Chem. Soc.* **2011**, *133*, 15506.
(22) Liu, Y. L.; Eubank, J. F.; Cairns, A. J.; Eckert, J.; Kravtsov, V. C.; Luebke, R.; Eddaoudi, M. *Angew. Chem., Int. Ed.* **2007**, *46*, 3278.
(23) Moellmer, J.; Celer, E. B.; Luebke, R.; Cairns, A. J.; Staudt, R.; Eddaoudi, M.; Thommes, M. *Microporous Mesoporous Mater.* **2010**, *129*, 345.
(24) Belof, J. L.; Stern, A. C.; Eddaoudi, M.; Space, B. *J. Am. Chem. Soc.* **2007**, *129*, 15202.
(25) Yang, H. G.; Zeng, H. C. *Angew. Chem., Int. Ed.* **2004**, *43*, 5206.
(26) Liu, B.; Zeng, H. C. *J. Am. Chem. Soc.* **2004**, *126*, 16744.
(27) Liu, B.; Zeng, H. C. *J. Am. Chem. Soc.* **2004**, *126*, 8124.